Journal of Mechanical Design | Volume 130 | Issue 1 | Research Paper

Saddlepoint Approximation for Sequential Optimization and Reliability Analysis

Xiaoping Du

Assistant Professor

Department of Mechanical and Aerospace Engineering

University of Missouri – Rolla

Rolla, Missouri 65409 – 4494

Phone: (573) 341-7249

E-mail: dux@umr.edu

Submitted on January 11, 2006

Revised on May 17, 2006

Revised on August 14, 2006

Revised on September 3, 2006

Abstract

A good balance between accuracy and efficiency is essential for reliability-based design (RBD). For this reason, sequential-loops formulations combined with the First Order Reliability Method (FORM) are usually used. FORM requires a nonlinear nonnormal-to-normal transformation, which may increase the nonlinearity of a probabilistic constraint function significantly. The increased nonlinearity may lead to an increased error in reliability estimation. In order to improve accuracy and maintain high efficiency, the proposed method uses the accurate Saddlepoint Approximation for reliability analysis. The overall RBD is conducted in a sequence of cycles of deterministic optimization and reliability analysis. The reliability analysis is performed in the original random space without any nonlinear transformation. As a result, the proposed method provides an alternative approach to RBD with higher accuracy when the nonnormal-to-normal transformation increases the nonlinearity of probabilistic constraint functions.

1. Introduction

Reliability-based design (RBD) ensures that the probability of failure be invariably small in the presence of uncertainty. RBD has been used in engineering fields for several decades [1], including those in civil, mechanical, and aerospace engineering.

In RBD, the trade-off between higher reliability and a lower cost is usually sought. The cost-type objective is minimized while reliability constraints are maintained. A RDB optimizer calls reliability analysis repeatedly to assess if the reliability requirement is met. The First Order Reliability Method (FORM) [2] is typically used for the reliability assessment, which is formulated as another optimization problem. Because of the double-loop nature as shown in Fig.1, RBD is computationally expensive.

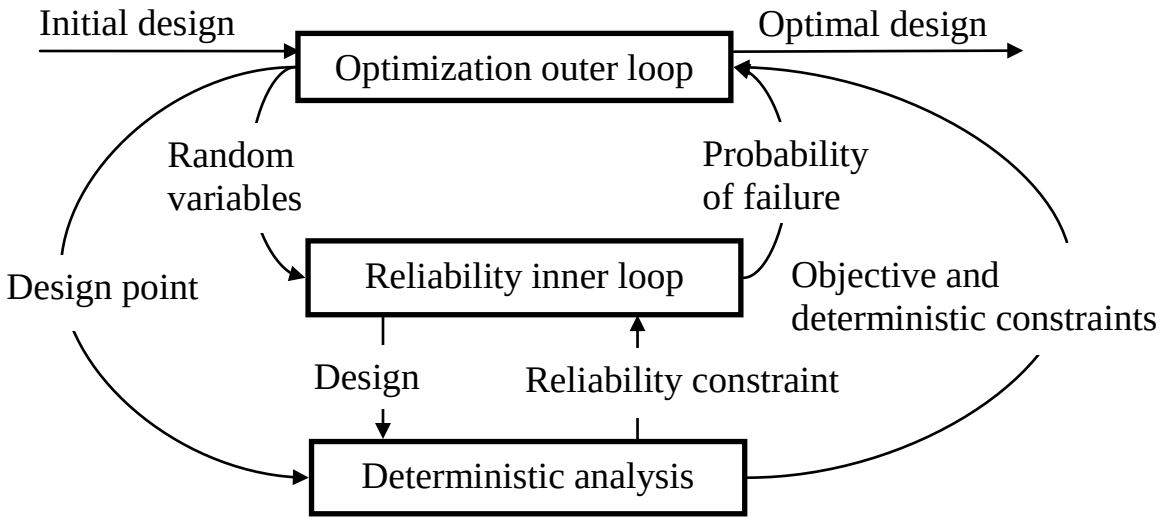

Fig. 1 Double-loop RBD

To reduce the computational cost, the sequential loops RBD methods in conjunction with FORM have been developed. The high efficiency is achieved in the following two aspects.

1) Decouple reliability analysis from deterministic optimization

Sequential cycles are employed. In each cycle, optimization and reliability analysis are decoupled; reliability analysis is conducted after optimization. The procedure is illustrated in Fig.

2. Since the process is expected to converge with a few cycles, the efficiency is much higher than the double-loop procedure schematized in Fig. 1.

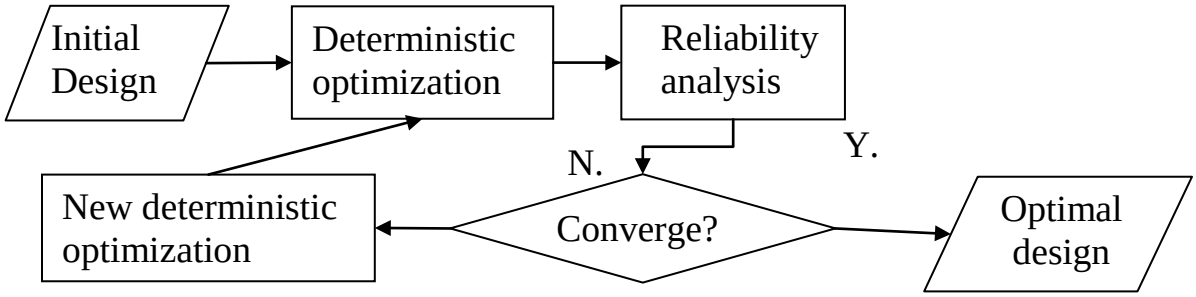

Fig 2. Sequential loops procedure

The typical sequential loops method is the safety-factor based method [3]. Other methods include the single-loop single variable method [4], sequential optimization and reliability assessment (SORA) [5, 6], and other variations [7, 8]. The methods differ from each other in whether random design variables are included, whether the MPP is searched, and whether the full reliability analysis is performed for inactive probabilistic constraints [9, 10]. SORA is a generic method because it contains both deterministic and random design variables, as well as random parameters. Various reliability analysis methods, such as FORM, the use of KKT conditions for the MPP, and the moment matching method, can be used in SORA. In this paper, we use SORA due to its generality.

(2) Perform reliability analysis only up to the necessary level

Calculating a specific value of a probabilistic constraint that corresponds to the required reliability is the task of the inverse reliability analysis [11]. Such a value is termed as a percentile performance or performance measure [12]. In general, using the percentile performance is more efficient than using the actual reliability in RBD [12, 13].

Even though FORM is efficient, it may not be accurate. It requires nonnormal random variables be transformed into standard normal variables. In the transformed random space a

probabilistic constraint function is linearized at the so called Most Probable Point (MPP). The nonnormal-to-normal transformation is nonlinear and may increase the nonlinearity of a constraint function [14]. In this case, FORM will result in a large error in reliability estimation.

The First Order Saddlepoint Approximation (FOSPA) eliminates the nonlinear transformation [21]. It linearizes a probabilistic constraint function in the original random space. And then the accurate Saddlepoint Approximation is employed. FOSPA produces more accurate reliability estimation than FORM does when the latter increases the nonlinearity of a constraint function [21]. In this work, we integrate FOSPA with SORA to provide an alternative RBD method when FORM is not appropriate. The new method is therefore termed as SORA-SPA.

FOSPA is designed for only reliability calculation, but SORA uses a percentile performance formulation. Directly calculating a percentile performance by FOSPA would require an iterative process and would not be efficient. Therefore, the research issue is to modify FOSPA so that it can evaluate the percentile performance efficiently. A computational procedure and algorithms are developed. Details of the procedure and algorithms are discussed in Section 4 after the introduction to the general RBD model and saddlepoint approximation in Sections 2 and 3. Four examples are then presented in Section 5 followed by conclusions in Section 6.

2. Model of Reliability-Based Design

A typical RBD model is given by

$$\begin{cases} \underset{(\mathbf{d},\boldsymbol{\mu}_\mathbf{X})}{\text{Min}}\ f(\mathbf{d},\boldsymbol{\mu}_\mathbf{X},\boldsymbol{\mu}_\mathbf{P}) \\ s.t. \\ \Pr\{G_i(\mathbf{d},\mathbf{X},\mathbf{P}) \le 0\} \ge [R_i] = 1-\left[\, p_{fi} \,\right],\ i = 1,2,\cdots,n_G \\ g_j(\mathbf{d},\boldsymbol{\mu}_\mathbf{X},\boldsymbol{\mu}_\mathbf{P}) \le 0,\ j = 1,2,\cdots,n_g \end{cases} \tag{1}$$

In the above model, $\mathbf{X} = (X_1, X_2, \cdots, X_n)$ is the vector of independent random design variables whose mean values $\boldsymbol{\mu}_X = (\mu_{X1}, \mu_{X2}, \cdots, \mu_{Xn})$ are to be determined; and *n* is the number of random design variables. $\mathbf{P} = (P_1, P_2, \cdots, P_m)$ is the vector of independent random parameters (noise factors), which can not be controlled by designers; and *m* is the number of the random parameters. $f(\cdot)$ is the objective function and is evaluated at the means of **X** and **P**, $\boldsymbol{\mu}_X = (\mu_{X1}, \mu_{X2}, \cdots, \mu_{Xn})$ and $\boldsymbol{\mu}_P = (\mu_{P1}, \mu_{P2}, \cdots, \mu_{Pm})$, respectively. $G_i(\mathbf{d}, \mathbf{X}, \mathbf{P})$ $(i = 1, 2, \cdots, n_G)$ are probabilistic constraint functions whose probability of constraint satisfaction or reliability, $R_i = \Pr\{G_i(\mathbf{d}, \mathbf{X}, \mathbf{P}) \le 0\}$, should be greater than or equal to the required reliability $[R_i]$. $\left[p_{fi} \right]$ is the allowable probability of failure for constraint *i*. $g_j(\mathbf{d}, \boldsymbol{\mu}_\mathbf{X}, \boldsymbol{\mu}_\mathbf{P})$ $(j = 1, 2, \cdots, n_g)$ are deterministic constraint functions and are evaluated at the means of random variables.

As mentioned previously, the percentile formulation is usually used due to its efficiency. By definition, if the percentile performance that corresponds to the required reliability $[R_i] = 1 - [p_{fi}]$ is $G_i^{1-[p_{fi}]}$, then

$$\Pr\{G_i(\mathbf{d}, \mathbf{X}, \mathbf{P}) \le G_i^{1-[p_{fi}]}\} = 1 - [p_{fi}]. \tag{2}$$

Eq. 2 implies that the reliability requirement $\Pr\{G_i(\mathbf{d}, \mathbf{X}, \mathbf{P}) \le 0\} \ge 1 - \left[p_{fi} \right]$ will be satisfied if $G_i^{1-[p_{fi}]} \le 0$. Therefore, with the percentile performance, the equivalent RBD model becomes

$$\begin{cases} \underset{(\mathbf{d}, \boldsymbol{\mu}_\mathbf{X})}{\text{Min}} \; f(\mathbf{d}, \boldsymbol{\mu}_\mathbf{X}, \boldsymbol{\mu}_\mathbf{P}) \\ s.t. \\ G_i^{1-[p_f]}(\mathbf{d}, \mathbf{X}, \mathbf{P}) \le 0, \; i = 1, 2, \cdots, n_G \\ g_j(\mathbf{d}, \boldsymbol{\mu}_\mathbf{X}, \boldsymbol{\mu}_\mathbf{P}) \le 0, \; j = 1, 2, \cdots, n_g \end{cases} \tag{3}$$

When FORM is used, the percentile performance can be calculated at the MPP, $(\mathbf{X}_i^*, \mathbf{P}_i^*)$, of $G_i(\mathbf{d}, \mathbf{X}, \mathbf{P})$ as [12, 13]

$$G_i^{1-[p_{fi}]}(\mathbf{d}, \mathbf{X}, \mathbf{P}) = G_i(\mathbf{d}, \mathbf{X}_i^*, \mathbf{P}_i^*), \tag{4}$$

where $\mathbf{X}_i^*$ and $\mathbf{P}_i^*$ are the components of the MPP for the *i*-th reliability constraint function $G_i(\mathbf{d}, \mathbf{X}, \mathbf{P})$. The RBD model is then given by

$$\begin{cases} \underset{(\mathbf{d}, \boldsymbol{\mu}_\mathbf{X})}{\text{Min}} \ f(\mathbf{d}, \boldsymbol{\mu}_\mathbf{X}, \boldsymbol{\mu}_\mathbf{P}) \\ s.t. \\ G_i(\mathbf{d}, \mathbf{X}_i^*, \mathbf{P}_i^*) \le 0, \ i = 1, 2, \cdots, n_G \\ g_j(\mathbf{d}, \boldsymbol{\mu}_\mathbf{X}, \boldsymbol{\mu}_\mathbf{P}) \le 0, \ j = 1, 2, \cdots, n_g \end{cases} \tag{5}$$

SORA [5] solves the above RBD model sequentially starting from the first cycle where the deterministic optimization is performed at the means of random variables. FORM is then used to find the MPP $(\mathbf{X}_i^*, \mathbf{P}_i^*)$ at the optimal point. In the second cycle, the MPP $(\mathbf{X}_i^*, \mathbf{P}_i^*)$ is used to formulate a new (modified) deterministic optimization problem. The reliability analysis is performed again after the modified deterministic optimization problem is solved. This process repeats till convergence.

3. The First Order Saddlepoint Approximation

Saddlepoint Approximation (SPA) provides an accurate estimate of the cumulative distribution function (CDF) in a tail area [15-26]. The first application of SPA in reliability analysis was the work of the Second Order Reliability Method (SORM) by Tvedt [24]. After a performance function is approximated in a quadratic form at the MPP, SPA is applied to calculate the reliability. This method is more accurate than the original SORM, but is inefficient because of the use of second derivatives. An efficient and accurate First Order Saddlepoint

Approximation (FOSPA) has been proposed recently [14]. A brief introduction to FOSPA is given below.

Since there is no need to distinguish the random design variables **X** from the random parameters **P** in reliability analysis, we use a vector **Y** to represent all the random variables, namely,

$$\mathbf{Y} = (\mathbf{X}, \mathbf{P}). \tag{6}$$

For brevity, we also omit the subscript for a probabilistic function and use $G(\mathbf{X}, \mathbf{P}) = G(\mathbf{Y})$ to denote an arbitrary probabilistic constraint function. Different from FORM where the constraint function is linearized in the transformed space, in FOSPA, $G(\mathbf{Y})$ is linearized in the original random space. The expansion point is called the Most Likelihood Point (MLP) [14], $\underset{\wedge}{\mathbf{y}} = (\underset{\wedge}{\mathbf{x}}, \underset{\wedge}{\mathbf{p}})$, which is on the limit state $G(\mathbf{Y}) = 0$. The linearization is given by

$$G(\mathbf{Y}) \approx \nabla(\underset{\wedge}{\mathbf{y}})^{\mathrm{T}} (\mathbf{Y} - \underset{\wedge}{\mathbf{y}}) = \sum_{j=1}^{m+n} \left. \frac{\partial G}{\partial Y_j} \right|_{\underset{\wedge}{\mathbf{y}}} (Y_j - \underset{\wedge}{y}_j), \tag{7}$$

where $\nabla(\underset{\wedge}{\mathbf{y}})$ is the gradient of $G(\mathbf{Y})$ at $\underset{\wedge}{\mathbf{y}} = (\underset{\wedge}{\mathbf{x}}, \underset{\wedge}{\mathbf{p}})$.

At the MLP, the joint probability density function (PDF) has its highest value; therefore, the following model is used to identify the MLP $\underset{\wedge}{\mathbf{y}} = (\underset{\wedge}{\mathbf{x}}, \underset{\wedge}{\mathbf{p}})$,

$$\begin{cases} \max\limits_{\mathbf{y}} \quad \prod\limits_{j=1}^{m+n} f_j(y_j) \\ \text{s.t.} \quad G(\mathbf{y}) = 0 \end{cases} \tag{8}$$

where $f_j(y_j)$ is the probability density function (PDF) of Y_j, and $\prod\limits_{i=1}^{m+n} f_j(y_j)$ is the joint PDF of the independent random variables $\mathbf{Y} = (\mathbf{X}, \mathbf{P})$.

Linearizing $G(\mathbf{Y})$ at the MLP results in the minimum accuracy loss due to the linearization [14]. After the constraint function is approximated by Eq. 7, SPA is used to estimate the reliability or the probability of failure.

Let the cumulant generating function (CGF) of Y_j be $K_{yj}(t)$, based on Eq. 7, the CGF of $G(\mathbf{Y})$ is given by [27]

$$K_G(t) = \sum_{j=1}^{m+n} K_{yj}\left(\left. \frac{\partial G}{\partial Y_j} \right|_{\hat{\mathbf{y}}} t \right). \tag{9}$$

The saddlepoint t_s is the solution to the following equation

$$K_G^{'}(t) = 0. \tag{10}$$

According to Lugannani and Rice's formula [18], the reliability is approximated by

$$R = \Pr\{G \le 0\} = \Phi(w) + \phi(w)\left(\frac{1}{w} - \frac{1}{v}\right), \tag{11}$$

where $\Phi(\cdot)$ and $\phi(\cdot)$ are the CDF and PDF of a standard normal distribution, respectively;

$$w = sgn(t_s)\left\{2\left[-K(t_s)\right]\right\}^{1/2} \tag{12}$$

and

$$v = t_s\left[K^{"}(t_s)\right]^{1/2}, \tag{13}$$

where $sgn(t_s)$ = +1, -1, or 0, depending on whether t_s is positive, negative or zero.

The central idea of SPA is that the probability integration is approximated at the saddlepoint where the integrand has the highest contribution. SPA has several excellent features. It yields extremely accurate probability estimation, especially in the tail area of a distribution [16, 23]. It requires only a process of finding one saddlepoint without any integration. For the complete methodology, interested readers may refer to [22].

4. Reliability-Based Design with Saddlepoint Approximation

4.1 Overview

In the proposed SORA-SPA method, after deterministic optimization, reliability analysis is performed, where the MLPs corresponding to the required reliability are searched. Then in the next cycle, the modified deterministic optimization is formulated using the MLPs. The process is outlined in Fig. 3.

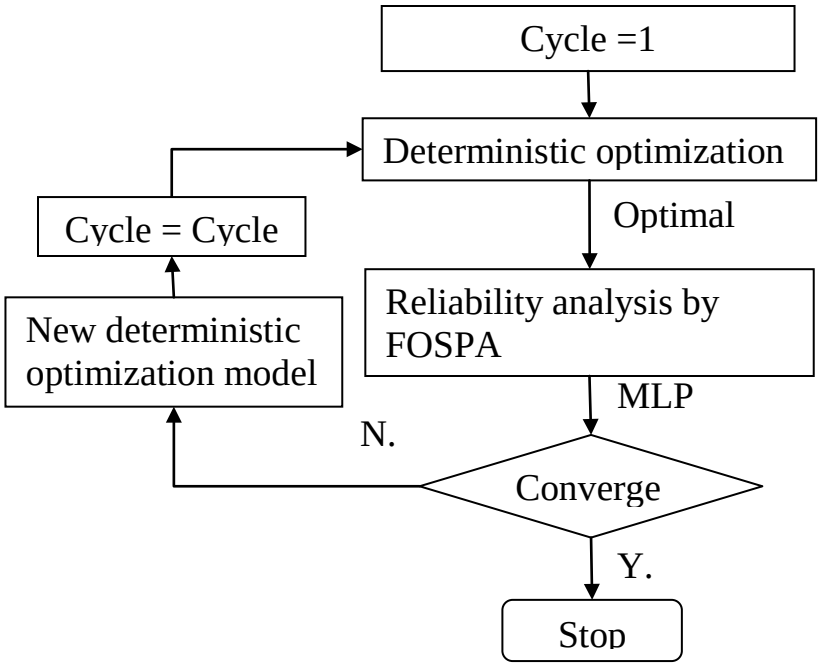

Fig. 3 Outline of the SORA-SPA process

4.2 Reliability analysis

The purposes of reliability analysis in the proposed method are 1) to calculate the percentile performance and 2) to provide information for building a new (modified) deterministic optimization model. The original FOSPA method is only for reliability calculation and is not intended to compute the percentile performance. The direct use of FOSPA is computationally expensive; we therefore propose an efficient approach to calculating the percentile performance.

The magnitudes of random variables may be in substantially different orders. For example, a material strength is in megapascals (MPa), and a diameter of a shaft is in millimeters (mm). To maintain numerical stability, we use the standardized random variables. A standardized variable is defined by

$$Z = \frac{Y - \mu_Y}{\sigma_Y}, \tag{14}$$

where μ_Y and σ_Y are the mean and standard deviation of *Y*, respectively.

The probabilistic constraint function is then expressed in terms of the standardized variables as

$$G(\mathbf{d}, \mathbf{Y}) = G(\mathbf{d}, \mathbf{Z}) = G(\mathbf{d}, \mathbf{Z}_X, \mathbf{Z}_P). \tag{15}$$

It should be noted that the transformation in Eq. 14 is linear and does not increase the nonlinearity of a probabilistic constraint function after the transformation.

The CGF of several distributions are given in Table 1.

Table 1 CGF of some distributions

Distribution	PDF	CGF	
Normal	$f(x) = \frac{1}{\sqrt{2\pi}\sigma} e^{-\frac{(x-\mu)^2}{2\sigma^2}}$	$K_X(t) = \mu t + \frac{1}{2}\sigma^2 t^2$	$K_Z(t) = \frac{1}{2}t^2$
Exponential	$f(x) = \beta e^{-\beta x}$	$K_X(t) = -\ln\left(1 - \frac{t}{\beta}\right)$	$K_Z(t) = -t - \ln(1-t)$
Uniform	$f(x) = \frac{1}{b-a}$	$K_X(t) = \ln\left(\frac{e^{bt} - e^{at}}{(b-a)t}\right)$	$K_Z(t) = \ln\left(\frac{e^{\sqrt{3}t} - e^{-\sqrt{3}t}}{2\sqrt{3}t}\right)$
Type I Extreme Value (Gumbel)	$f(x) = \frac{1}{\sigma} e^{-\frac{x-\alpha}{\beta}} \exp\left(-e^{-\frac{x-\alpha}{\beta}}\right)$	$K_X(t) = \alpha t + \ln\Gamma(1-\beta t)$	$K_Z(t) = \frac{\mu_X - \alpha}{\sigma_X} t + \ln\Gamma(1 - \frac{\beta}{\sigma_X} t)$
χ^2	$f(x) = \frac{1}{\Gamma(n/2)2^{n/2}} x^{n/2-1} e^{-\frac{1}{2}x}$	$K_X(t) = -\frac{1}{2} n \ln(1-2t)$	$K_Z(t) = -\frac{\mu_X}{\sigma_X} t - \frac{1}{2} n \ln\left(1 - 2\frac{t}{\sigma_X}\right)$
Gamma	$f(x) = \frac{\beta^\alpha}{\Gamma(\alpha)} x^{\alpha-1} e^{-\beta x}$	$K_X(t) = -\alpha \ln(1 - t/\beta)$	$K_Z(t) = -\frac{\mu_X}{\sigma_X} t - \alpha \ln\left(1 - \frac{t}{\sigma_X \beta}\right)$

Since we expect reliability constraints to be satisfied only at the end of the optimization process, we do not need to calculate the exact percentile performance in each cycle. We therefore propose the following reliability analysis procedure, which ensures that the reliability requirement be satisfied at the final optimal point. The reliability analysis in the *k*-th cycle is explained below.

1) Search the MLP at the optimal point $(\mathbf{d}^k, \boldsymbol{\mu}_X^k)$.

The MLP $(\underset{\wedge}{\mathbf{z}}_X^{k,i}, \underset{\wedge}{\mathbf{z}}_P^{k,i})$ of the *i*-th constraint function G_i $(i = 1, 2, \cdots, n_G)$ at the limit state $G_i = 0$ is the solution to the following optimization model

$$\begin{cases} \max\limits_{\mathbf{z}_X, \mathbf{z}_P} \prod\limits_{j=1}^{m+n} f_{zj}(z_j) \\ \text{s.t.} \quad G_i(\mathbf{d}^k, \mathbf{z}_X, \mathbf{z}_P) = 0 \end{cases} \tag{16}$$

The superscript *k* in the MLP $\underset{\wedge}{\mathbf{z}}^{k,i} = (\underset{\wedge}{\mathbf{z}}_X^{k,i}, \underset{\wedge}{\mathbf{z}}_P^{k,i})$ denotes the *k*-th cycle and the superscript *i* denotes the *i*-th constraint.

2) Linearize $G_i(\mathbf{d}, \mathbf{X}, \mathbf{P})$ at the MLP $\underset{\wedge}{\mathbf{z}}^{k,i} = (\underset{\wedge}{\mathbf{z}}_X^{k,i}, \underset{\wedge}{\mathbf{z}}_P^{k,i})$.

$$\begin{aligned} G_i(\mathbf{d}^k, \mathbf{Z}) &\approx \nabla(\underset{\wedge}{\mathbf{z}}^{k,i})^{\mathrm{T}}(\mathbf{Z} - \underset{\wedge}{\mathbf{z}}^{k,i}) = \sum_{j=1}^{m+n} \left.\frac{\partial G_i}{\partial Z_j}\right|_{\underset{\wedge}{\mathbf{z}}^{k,i}} (Z_j - \underset{\wedge}{z}_j^{k,i}) = -\sum_{j=1}^{m+n} \left.\frac{\partial G_i}{\partial Z_j}\right|_{\underset{\wedge}{\mathbf{z}}^{k,i}} \underset{\wedge}{z}_j^{k,i} + \sum_{j=1}^{m+n} \left.\frac{\partial G_i}{\partial Z_j}\right|_{\underset{\wedge}{z}_j^{k,i}} Z_j \\ &= a_0 + \sum_{j=1}^{m+n} a_j Z_j, \end{aligned} \tag{17}$$

where the coefficients are

$$a_0 = -\sum_{j=1}^{m+n} \left.\frac{\partial G_i}{\partial Z_j}\right|_{\underset{\wedge}{\mathbf{z}}^{k,i}} \underset{\wedge}{z}_j^{k,i}, \tag{18}$$

and

$$a_j = \left.\frac{\partial G_i}{\partial Z_j}\right|_{\hat{z}_j^{k,i}}. \tag{19}$$

3) Find the percentile performance $G_i^{1-[p_{fi}]}$ and the MLP $(\hat{\mathbf{z}}_X^{k,i}, \hat{\mathbf{z}}_P^{k,i})$ corresponding to the required reliability $1-[p_{f_i}]$.

According to Eq.2, the percentile performance $G_i^{1-[p_{fi}]}$ is the solution to the following equation.

$$\Pr\left\{a_0 + \sum_{j=1}^{m+n} a_j Z_j \le G_i^{1-[p_{fi}]}\right\} = 1-[p_{fi}]. \tag{20}$$

The reliability on the left-hand side of Eq. 20 is calculated with FOSPA as follows.

Let

$$\widehat{G}_i = a_0 + \sum_{j=1}^{m+n} a_j Z_j - G_i^{1-[p_{fi}]}. \tag{21}$$

The CGF of $\widehat{G}_i$ can be derived as [22]

$$K_{\widehat{G}_i}(t) = \left(a_0 - G_i^{1-[p_{fi}]}\right)t + \sum_{j=1}^{m+n} K_{Z_j}\left(a_j t\right). \tag{22}$$

where K_{Z_j} is the CGF of Z_j, which is given in Table 1.

According to Eq. 10, the saddlepoint t_s is the solution to the following equation

$$K'_{\widehat{G}_i}(t) = \left(a_0 - G_i^{1-[p_{fi}]}\right) + a_j \sum_{j=1}^{m+n} K'_{Z_j}\left(a_j t\right) = 0. \tag{23}$$

Thereafter, the probability $\Pr\left\{a_0 + \sum_{j=1}^{m+n} a_j Z_j - G_i^{1-[p_{fi}]} \le 0\right\} = \Pr\left\{\widehat{G}_i \le 0\right\}$ in Eq. 20 can be easily calculated with Eqs. 11 through 13.

Newton's method or bisection method [28] can be used to solve Eq. 23. The percentile performance $G_i^{1-[p_{fi}]}$ will be used to find the corresponding MLP $(\hat{\mathbf{z}}_X^{k,i}, \hat{\mathbf{z}}_P^{k,i})$. And then $(\hat{\mathbf{z}}_X^{k,i}, \hat{\mathbf{z}}_P^{k,i})$ will be used to formulate the reliability constraints G_i in the next (k+1)-th cycle. The MLP $(\hat{\mathbf{z}}_X^{k-1,i}, \hat{\mathbf{z}}_P^{k-1,i})$ can be found at the percentile performance $G_i^{1-[p_{fi}]}$ with the following model.

$$\begin{cases} \max\limits_{\mathbf{z}_X, \mathbf{z}_P} \prod\limits_{j=1}^{m+n} f_{zj}(z_j) \\ \text{s.t.} \quad \widehat{G}_i = a_0 + \sum\limits_{j=1}^{m+n} a_j Z_j - G_i^{1-[p_{fi}]} = 0 \end{cases} \tag{24}$$

Any optimization algorithm can be used to solve the above model. It should be noted that solving the above model and Eq. 20 does not call the constraint function G_i. It is also worthwhile to note that the MLP $\underset{\wedge}{\mathbf{z}}^{k,i} = (\underset{\wedge X}{\mathbf{z}}^{k,i}, \underset{\wedge P}{\mathbf{z}}^{k,i})$ (the solution to Eq. 20) is for the limit state $G_i = 0$ and that the MLP $(\hat{\mathbf{z}}_X^{k,i}, \hat{\mathbf{z}}_P^{k,i})$ (the solution to Eq. 24) is for the percentile performance $G_i^{1-[p_{fi}]}$. Only the latter is used to formulate a modified deterministic optimization model for the next cycle.

In summary, the purpose of reliability analysis is to provide information so that a new optimization model can be formulated for the next cycle. Two steps are involved. (1) The MLP $(\underset{\wedge X}{\mathbf{z}}^{k,i}, \underset{\wedge P}{\mathbf{z}}^{k,i})$ for $G_i = 0$ is first identified, then G_i is linearized at $(\underset{\wedge X}{\mathbf{z}}^{k,i}, \underset{\wedge P}{\mathbf{z}}^{k,i})$. The FOSPA is used to calculate the percentile performance $G_i^{1-[p_{fi}]}$ at $(\underset{\wedge X}{\mathbf{z}}^{k,i}, \underset{\wedge P}{\mathbf{z}}^{k,i})$. (2) The MLP $(\hat{\mathbf{z}}_X^{k,i}, \hat{\mathbf{z}}_P^{k,i})$ at $G_i^{1-[p_{fi}]}$ is identified. It is obvious that the percentile performance $G_i^{1-[p_{fi}]}$ is the function value of G_i at the MLP $(\hat{\mathbf{z}}_X^{k,i}, \hat{\mathbf{z}}_P^{k,i})$. To satisfy the reliability requirement for G_i, the percentile performance $G_i^{1-[p_{fi}]}$

should be less than zero, namely, $G_i^{1-[p_{fi}]} = G_i(\mathbf{d}, \hat{\mathbf{z}}_X^{k,i}, \hat{\mathbf{z}}_P^{k,i}) \le 0$. This condition is used to formulate new reliability constraint functions in the (k+1)-th cycle.

The reliability analysis is demonstrated with a special two-dimensional problem in Fig. 4, where the constraint function G_i contains two standardized random variables Z_1 and Z_2. At first, the constraint function is linearized at the optimization point obtained from the k-th optimization. Then the MLP $\underset{\wedge}{\mathbf{z}}^{k,i}$ is searched by maximizing the joint PDF at $G_i = 0$. Next, the constraint function is liearized at $\underset{\wedge}{\mathbf{z}}^{k,i}$, and the percentile performance $G_i^{1-[p_{fi}]}$ is calculated based on the linearization. Finally, the MLP $\hat{\mathbf{z}}^{k,i}$ is identified. The joint PDF at $\underset{\wedge}{\mathbf{z}}^{k,i}$ has the highest value at the line $a_0 + a_1\left(Z_1 - \hat{z}_1^{k,i}\right) + a_2\left(Z_2 - \hat{z}_2^{k,i}\right) = G_i^{1-[p_{fi}]}$. $\underset{\wedge}{\mathbf{z}}^{k,i}$ will then be used to formulate a new (modified) deterministic optimization model for the (k+1)-th cycle.

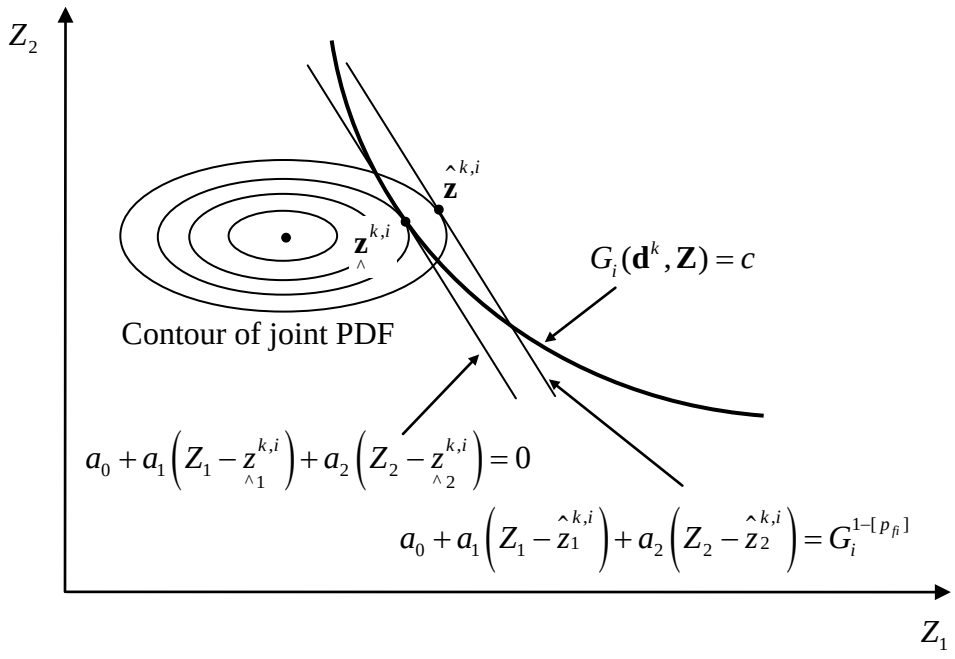

Fig. 4 Reliability analysis

4.3 Optimization

We have discussed the reliability analysis in the *k*-th cycle. Next we discuss how to formulate the modified deterministic optimization for the (*k*+1)-th cycle. The percentile formulation in Eq. 3 is used to formulate a RBD problem. As discussed in the last subsection, the percentile performances of probabilistic constraints G_i $(i=1,2,\cdots,n_G)$ are calculated at the MLPs $(\hat{\mathbf{x}}^{k,i},\hat{\mathbf{p}}^{k,i})$ as

$$G_i^{1-[p_{fi}]}=G_i\left(\mathbf{d},\hat{\mathbf{x}}^{k,i},\hat{\mathbf{p}}^{k,i}\right)=G_i\left(\mathbf{d},\boldsymbol{\mu}_X+\boldsymbol{\sigma}_X^{\mathrm{T}}\hat{\mathbf{z}}_X^{k,i},\boldsymbol{\mu}_P+\boldsymbol{\sigma}_P^{\mathrm{T}}\hat{\mathbf{z}}_P^{k,i}\right). \tag{25}$$

The RBD optimization in (*k*+1)-th cycle is then modeled as

$$\begin{cases}\underset{(\mathbf{d},\boldsymbol{\mu}_\mathbf{X})}{\mathrm{Min}}\ f(\mathbf{d},\boldsymbol{\mu}_\mathbf{X},\boldsymbol{\mu}_\mathbf{P})\\ s.t.\\ G_i\left(\mathbf{d},\boldsymbol{\mu}_X+\boldsymbol{\sigma}_X^{\mathrm{T}}\hat{\mathbf{z}}_X^{k,i},\boldsymbol{\mu}_P+\boldsymbol{\sigma}_P^{\mathrm{T}}\hat{\mathbf{z}}_P^{k,i}\right)\le 0,\ i=1,2,\cdots,n_G\\ g_j(\mathbf{d},\boldsymbol{\mu}_\mathbf{X},\boldsymbol{\mu}_\mathbf{P})\le 0,\ j=1,2,\cdots,n_g\end{cases} \tag{26}$$

Because the following equation holds

$$\boldsymbol{\mu}_X+\boldsymbol{\sigma}_X^{\mathrm{T}}\hat{\mathbf{z}}_X^{k,i}=\boldsymbol{\mu}_X+\boldsymbol{\sigma}_X^{\mathrm{T}}\frac{\hat{\mathbf{x}}^{k,i}-\boldsymbol{\mu}_X^k}{\boldsymbol{\sigma}_X}=\boldsymbol{\mu}_X-\left(\boldsymbol{\mu}_X^k-\hat{\mathbf{x}}^{k,i}\right)=\boldsymbol{\mu}_X-\mathbf{s}^{k,i}\ , \tag{27}$$

where $\mathbf{s}^{k,i}$ is called the shifting vector and is given by

$$\mathbf{s}^{k,i}=\left(\boldsymbol{\mu}_X^k-\hat{\mathbf{x}}^{k,i}\right)\ , \tag{28}$$

the reliability constraint G_i in Eq. 26 becomes

$$G_i\left(\mathbf{d},\boldsymbol{\mu}_X-s^{k,i},\hat{\mathbf{p}}^{k,i}\right)\le 0\,. \tag{29}$$

Eq. 29 indicates that the reliability constraint G_i is evaluated at the MLP $\hat{\mathbf{p}}^{k,i}$ obtained in the previous cycle and that the constraint boundary in the design space is shifted toward the

feasible region with the distance $\mathbf{s}^{k,i}$. The distance is the difference between the design variables $\boldsymbol{\mu}_X^k$ and their MLP $\hat{\mathbf{x}}^{k,i}$.

The idea is illustrated in Fig. 5 where one reliability constraint function $G(X_1, X_2)$ with two random design variables is involved. The overall RBD starts from the deterministic optimization in the first cycle where the first optimal point $\boldsymbol{\mu}_X^1$ is found. The constraint is active because $\boldsymbol{\mu}_X^1$ is on the constraint boundary. In the reliability analysis, the constraint function is linearized at $\boldsymbol{\mu}_X^1$. Based on the linearization, the percentile performance $G^{1-[p_f]}$ is solved by Eq. 20, and the MLP $\hat{\mathbf{x}}^1$ is obtained from Eq. 24. In the second cycle, a modified deterministic optimization is formulated with shifted constraint boundary toward the feasible region by the distance $\mathbf{s}^1 = \left(\boldsymbol{\mu}_X^1 - \hat{\mathbf{x}}^1\right)$. The reliability will be improved at the optimal point $\boldsymbol{\mu}_X^2$ due to the reduced feasible region. After the optimization, reliability analysis is performed to obtain the MLP $\hat{\mathbf{x}}^2$ for the limit state $G = 0$. The constraint function is then linearized at $\hat{\mathbf{x}}^2$, and SPA is used to calculate the percentile performance $G^{1-[p_f]}$ and the MLP $\hat{\mathbf{x}}^2$. If the percentile performance $G^{1-[p_f]}$ is still greater than zero, the constraint boundary will be shifted again and the process will be repeated till convergence.

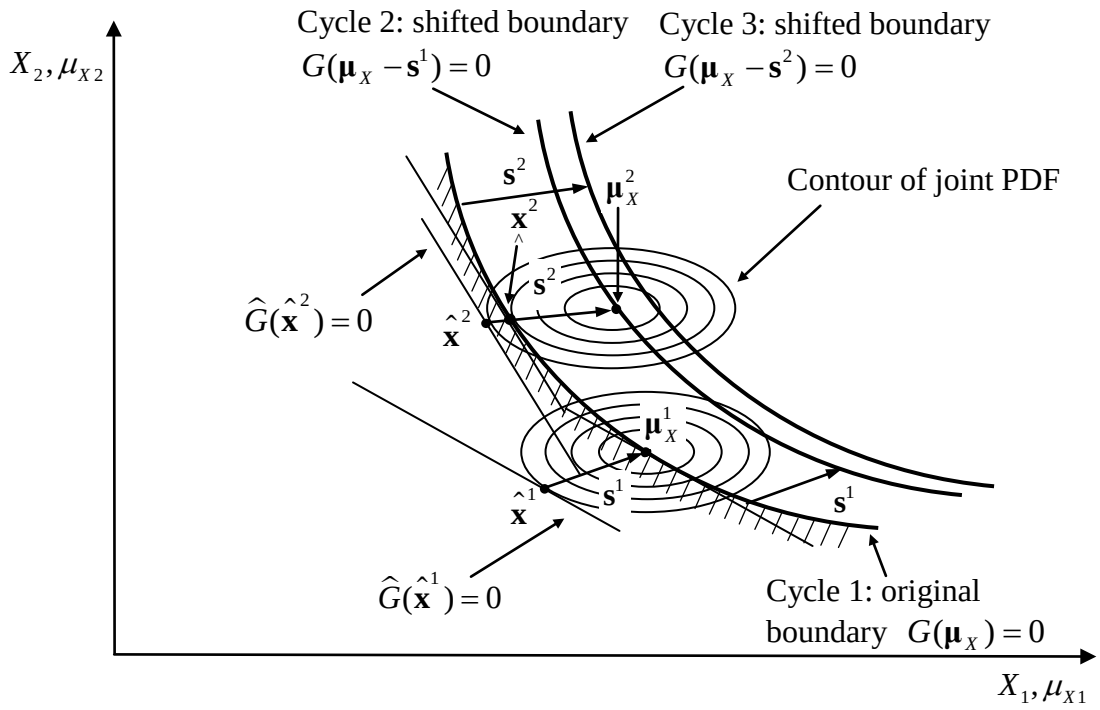

Fig. 5 Shifting constraint boundary

4.4 Numerical Implementations

In this work, the RBD optimization and the MLP search are performed with the Sequential Quadratic Programming (SQP). The equations of percentile performance and the saddlepoint are solved by the bisection method.

The stopping criteria of the overall RBD are as follows.

1) The reliability requirement is satisfied.

$$G_i^{1-[p_{fi}]} \le \varepsilon_1 \ (i = 1, 2, \cdots, n_G) \tag{30}$$

2) The difference of the objective functions in two consecutive cycles is small.

$$\left| f^k - f^{k-1} \right| \le \varepsilon_2 \tag{31}$$

where ε_1 and ε_2 are small positive numbers.

The proposed SORA-SPA method requires that a random variable is tractable; or in other words, a closed-form CGF exists. Some random variables may not have a closed-form CGF, for example, a Weibull distribution or a lognormal distribution. There are three ways to approach an intractable CGF: 1) Approximate the CGF using polynomial expansions [29]; 2) sample the intractable variable and use the samples to approximate the CGF [30]; and 3) transform the intractable random variable into another tractable random variable.

4.5 Selection of a RBD method

There is a fundamental difference between the proposed SORA-SPA method and a FORM based method. A probabilistic constraint function is linearized in the original random space in the former method while a probabilistic constraint function is linearized in the transformed space in the latter method. A question arises due to the difference: What method should be used for a given problem? The general answer would be as follows. If the nonnormal-to-normal transformation in FORM increases the nonlinearity of a probabilistic constraint function, the SPA method should be used; otherwise, FORM should be used. The nonlinearity can be measured by the curvature of the probabilistic constraint function at the MLP or MPP. The following two examples are used to demonstrate the idea. In example 1, the nonnormal-to-normal transformation increases nonlinearity of the probabilistic function, and the proposed method should be used. In example 2, the nonnormal-to-normal transformation decreases the nonlinearity of the probabilistic function, and FORM should be used.

In example 1, the constraint function is given by $G(\mathbf{Y}) = 40 - (Y_1 Y_2 + 8Y_1 + 8Y_2)$, where Y_1 and Y_2 follow an extreme value type I distribution (Gumbel distribution) with the mean of 1.5

and the standard deviation of 0.2. The probabilities of failure by FORM, FOSPA, and Monte Carlo simulation (MCS) with 10^6 samples are 0.00021331, 0.00040691, and 0.000363, respectively. Taking the MCS solution as a benchmark, FOSPA is more accurate than FORM. The reason is that FORM increases the nonlinearity of the function. This is illustrated in Figs. 6 and 7. The curvature of the function at the MLP in the original Y-space is 0.069338, and the curvature increases to -0.15703 at the MPP after the transformation in the standard normal U-space. The curve of $G(\mathbf{Y}) = 0$ in Fig. 6 is flatter than $G(\mathbf{U}) = 0$ in Fig. 7. In Fig. 6, the linearized function (a straight line) at the MLP in Y-space is plotted, and the linearized function at MPP in U-space, (which is a straight line in u-space in Fig. 7), is also plotted in Y-space where the line becomes a curve. It is shown in both figures that the constraint function is closer to the linearized function in Y-space. Therefore, the linearization in Y-space produces higher accuracy. In this case, SORA-SPA should be used.

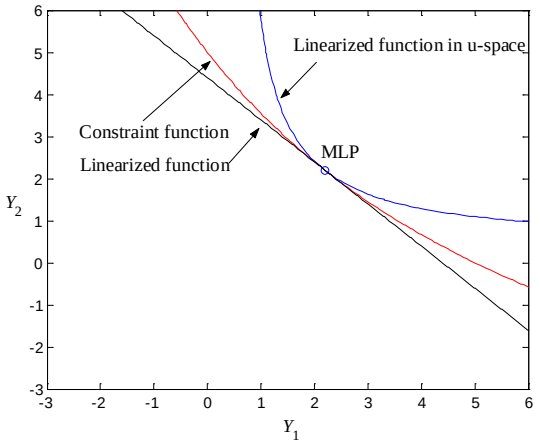

Fig. 6 Constraint function in y-space

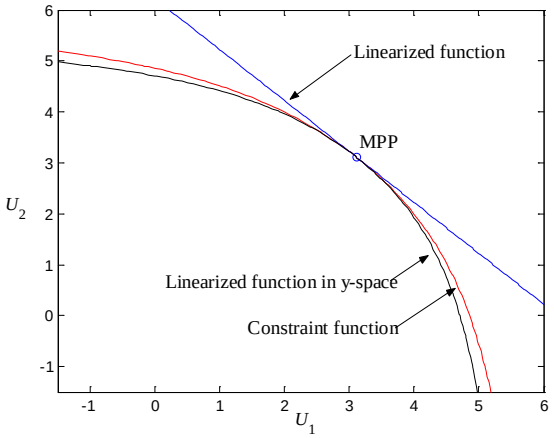

Fig. 7 Constraint function in u-space

In example 2, the constraint function is given by $G(\mathbf{Y}) = 4 - Y_1 Y_2$, where Y_1 and Y_2 follow the same distribution as in example 1. The probabilities of failure by FORM, FOSPA, and Monte Carlo simulation (MCS) with 10^6 samples are 0.0022882, 0.0038289, and 0.002717, respectively. Taking the MCS solution as the benchmark, FORM is more accurate than FOSPA. As shown in Figs. 8 and 9, the curvature of $G = 0$ is reduced significantly after the transformation, from 0.35355 at the MLP in Y-space to -0.045072 at the MPP in u-space. This indicates the reduced nonlinearity because of the transformation. In this case, SORA-FORM should be used.

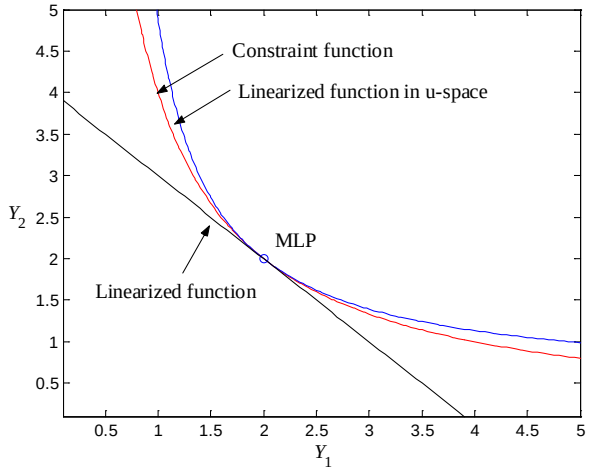

Fig. 8 Constraint function in y-space

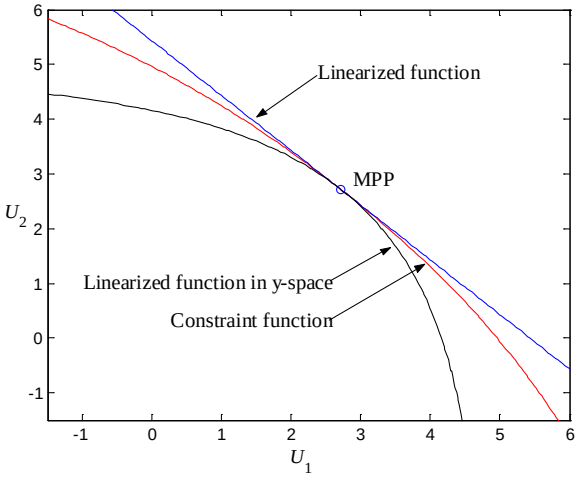

Fig. 9 Constraint function in u-space

It should be noted that the calculation of a curvature needs the second derivatives of a constraint function with respect to all its random variables. The recommendation is that calculate the curvatures at the MLP in Y-space and at the MPP in U-space after the first deterministic optimization is performed. If the curvature increases in U-space, one should use SORA-SPA method; otherwise, one should use SORA-FORM method. For a high-dimensional problem, principal curvatures may be used.

5. Examples

A number of problems have been used to test the proposed method. Four examples are presented here. These problems represent a wide range of application scenarios. Some problems have only deterministic design variables and only normal random variables, and others have both deterministic and random design variables, as well as nonnormal random variables. The accuracy and efficiency are compared between the proposed SORA-SPA method and SORA-FORM method [10]. The accuracy of the reliability calculation at the optimal point is confirmed with the result obtained from Monte Carlo simulation (MCS) with a large sample size, if no analytical solution exists. The efficiency is measured by the number of function evaluations, including those for both optimization and reliability analysis. The derivatives are evaluated numerically by the finite difference method. The MATLAB SQP optimizer is used for the optimization and reliability analysis. The same parameter setting and stopping criteria are used for both methods to ensure a fair comparison. It should be noted that the proposed method performs better than the FORM based RBD method in all the examples because FORM increases the nonlinearity of probabilistic constraint functions. The proposed method is not applicable when FORM decreases the nonlinearity of probabilistic constraint functions.

Example 1 – mathematical problem 1

In this problem, there are two deterministic design variables, $\mathbf{d} = (d_1, d_2)$, and *m* random parameters $\mathbf{P} = (P_1, P_2, \cdots, P_m)$. There is no random design variable. The RBD problem is modeled as

$$\begin{cases} \text{Min } f(\mathbf{d}) = d_1 d_2 \\ s.t. \\ \Pr\left\{ G(\mathbf{d},\mathbf{P}) = \sum_{i=1}^{m} P_i - (d_1 + d_2) \le 0 \right\} \ge 1 - [p_f] \\ d_1, d_2 \ge 0.01 \\ d_1, d_2 \le 100 \end{cases}$$

The allowable probability of failure is $[p_f] = 0.001$. Each of the independent random parameters follows a standard exponential distribution with the following CDF,

$$F_i(p_i) = 1 - \exp(-p_i).$$

The probability of failure for the constraint $G(\mathbf{d},\mathbf{P})$ from FORM and SPA can be found analytically for this specific mathematical problem. The accurate probability of failure is also available. Since the reliability analysis can be performed analytically, the RBD is conducted without sequential loops.

The optimal solutions for $m = 15$ using FORM, SPA, and analytical reliability analysis are displayed in Table 2. The results show that SPA produces a very accurate result, which is almost identical to the analytical result. The probability of failure at the optimal point from SPA is exactly at the required level, which is 0.01. The optimal solution from FORM has a large error. The actual probability of failure calculated at the optimal point from FORM is 0.02802, which is far away from the required probability of failure 0.01.

Table 2 Results from analytical methods

METHOD	$f(\mathbf{d})$	$\mathbf{d}^* = (d_1, d_2)$	p_f AT $\mathbf{d}^*$
FORM	134.96	(11.62, 11.62)	0.028
FSPA	222.79	(14.93, 14.93)	0.001
Theoretic solution	222.78	(14.93, 14.93)	0.001

The problem is also solved by SORA-FORM and SORA-SPA. The same results are obtained as shown in Table 2. The convergence history of each method and the number of

function evaluations are displayed in Tables 3 and 4, respectively. Both methods converge in three cycles (denoted by k in the table) but produce different solutions. At the optimal point, the percentile performance $G^{1-[p_f]}$ is close to zero for both methods. This indicates that the probabilistic constraint is active. It is also seen that the convergence is achieved progressively from the first cycle to the last. In Tables 3 and 4, N denotes the number of function evaluations (or deterministic analyses for evaluating objective function and all the constraint functions). SORA-SPA is more efficient than SORA-FORM since the former uses 111 function evaluations while the latter uses 254 function evaluations.

Table 3 Convergence history of SORA-FORM

k	$f(\mathbf{d})$	(d_1, d_2)	$g^{1-[p_f]}$	N
1	56.25	(7.5, 7.5)	14.85	
2	134.96	(11.62, 11.62)	0.0	254
3	134.96	(11.62, 11.62)	0.0	

Table 4 Convergence history of SORA-SPA

k	$f(\mathbf{d})$	(d_1, d_2)	$g^{1-[p_f]}$	N
1	56.25	(7.5, 7.5)	8.23	
2	222.79	(14.93, 14.93)	0.0	111
3	222.79	(14.93, 14.93)	0.0	

Example 2 – mathematical problem 2

In the previous example, no random design variable is involved, and therefore no constraint boundary shifting is needed. To test SORA-SPA for a more general case, in this problem, we use two deterministic design variables, $\mathbf{d} = (d_1, d_2)$, two random design variables $\mathbf{X} = (X_1, X_2)$, and eight random parameters $\mathbf{P} = (P_1, P_2, \cdots, P_8)$. The RBD problem is given by

$$\begin{cases} \text{Min } h(\mathbf{d}) = d_1 d_2 \mu_{X1} \mu_{X2} \\ s.t. \\ \Pr\left\{ G(\mathbf{P}) = \sum_{i=1}^{8} P_i - (d_1 + d_2 + \mu_{X1} + \mu_{X2}) \le 0 \right\} \ge 1 - [p_f] \\ d_1, d_2, \mu_{X1}, \mu_{X2} \ge 0.5 \\ d_1, d_2, \mu_{X1}, \mu_{X2} \le 10 \end{cases}$$

The allowable probability of failure is $[p_f] = 0.005$. Each of the independent random parameters follows a standard exponential distribution as in example 1.

The convergence history of each method is given in Tables 5 and 6. Since no analytical solution is available, Monte Carlo simulation (MCS) with 10^6 samples is used to calculate the actual probability of failure at the optimal points from SORA-FORM and SORA-SPA. The probability of failure calculated by MCS at the optimal point from SORA-FORM is $p_f = 0.0336$. It is much higher than the allowable probability of failure $[p_f] = 0.005$ with an error of $\varepsilon_{p_f} = 572.0\%$. The solution of SORA-FORM is therefore risky. The probability of failure calculated by MCS at the optimal point from SORA-SPA is $p_f = 0.0051$, which is very close to the allowable probability of failure $[p_f] = 0.005$. The error is $\varepsilon_{p_f} = 2\%$. SORA-FORM uses 361 function evaluations, and SORA-SPA uses 277 function evaluations. The results show that SORA-SPA is more accurate and efficient than SORA-FORM.

Table 5 Convergence history of SORA-FORM

k	$f(\mathbf{d})$	$(d_1, d_2, \mu_{x1}, \mu_{x2})$	$g^{1-[p_f]}$	p_f	ε_{p_f}	N
1	0.32	(0.75, 0.75, 0.75,0.75)	6.30			
2	4.04	(4.02, 4.02, 0.5, 0.5)	0.01	0.034	572.0%	361
3	4.05	(4.03, 4.03, 0.5, 0.5)	0.0			

* MCS solution p_f is from 10^6 samples, the error of the probability of failure under 95% confidence is 3.4%, and the 95% confidence interval is [0.031655, 0.033861].

Table 6 Convergence history of SORA-SPA

k	$f(\mathbf{d})$	$(d_1, d_2, \mu_{x1}, \mu_{x2})$	$g^{1-[p_f]}$	p_f	ε_{p_f}	N
1	0.32	(0.75, 0.75, 0.75, 0.75)	9.40			
2	92.24	(3.10, 3.10, 3.10, 3.10)	2.44			
3	11.96	(6.92, 6.92, 0.5, 0.5)	-2.57	5.1×10^{-3}	2.0%	277
4	7.92	(5.63, 5.63, 0.5, 0.5)	0.0			
5	7.92	(5.63, 5.63, 0.5, 0.5)	0.0			

* MCS solution is p_f from 10^6 samples, the error of the probability of failure under 95% confidence is 8.6%, and the 95% confidence interval is [0.004691, 0.005577].

Example 3 – cantilever beam design

In the previous two mathematical examples, there is only one constraint function, and the constraint function is linear. Next, we will test SORA-SPA using two engineering examples, which involve nonlinear constraint functions and different distributions.

A cantilever beam [3] to be designed is illustrated in Fig. 10.

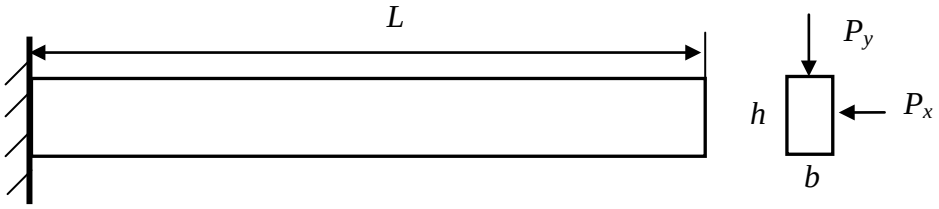

Fig. 10 Cantilever beam

The objective is to minimize the weight or equivalently the cross-area

$$f = \mu_b \mu_h ,$$

where b and h are random design variables, which represent the width and height of the cross section, respectively, and the design variables are their means $\mathbf{d} = (\mu_b, \mu_h)$. There is no

deterministic design variable in this problem. The random parameters are $\mathbf{P} = (P_x, P_y, E, S)$, which are the horizontal force, vertical force, Young's modulus, and material yield strength, respectively. Two cases with different distributions are considered. All the random variables are normally distributed in Case 1, and uniform distributions are involved in Case 2. The distributions of the random variables for both cases are shown in Tables 7 and 8, respectively.

Table 7 Distributions for Case 1

Variable	Mean	Standard deviation	Distribution
b	μ_b in	0.01 in	Normal
h	μ_h in	0.01 in	Normal
P_x	500 lb	100 lb	Normal
P_y	1000 lb	100 lb	Normal
E	29×10^6 psi	1.45×10^6 psi	Normal
S	40000 psi	2000 psi	Normal

Table 8 Distributions for Case 2

Variable	Parameter 1*	Parameter 2*	Distribution
b	μ_b in	0.01 in	Normal
h	μ_h in	0.01 in	Normal
P_x	300 lb	700 lb	Uniform
P_y	600 lb	1500 lb	Uniform
E	29×10^6 psi	1.45×10^6 psi	Normal
S	40000 psi	2000 psi	Normal

* Parameter 1 is the mean for a normal distribution and the lower bound for a uniform distribution. Parameter 2 is the standard deviation for a normal distribution and the upper bound for a uniform distribution

Two constraints are considered. The first constraint is that the maximum stress at the fixed end of the cantilever is less than the yield strength S.

$$G_1(\mathbf{d}) = \frac{6L}{bh}\left(\frac{P_x}{b} + \frac{P_y}{h}\right) - S \le 0,$$

where $L = 100$ in is the length of the beam.

The second constraint is that the tip displacement does not exceed an allowable value D_0,

$$G_2(\mathbf{d}) = \frac{4L^3}{E}\sqrt{\left(\frac{P_x}{b^3h}\right)^2 + \left(\frac{P_y}{bh^3}\right)^2} - D_0 \le 0$$

where $D_0 = 2.5$ in.

The allowable probability of failure of each of the reliability constraints is $[p_{f1}] = [p_{f2}] = 0.001$. The reliability-based design model is given by

$$\begin{cases} \underset{(\mu_b,\mu_h)}{\text{Min}}\ f = \mu_b\mu_h \\ \text{s.t.} \\ \quad \Pr\left\{G_1 = \dfrac{6L}{bh}\left(\dfrac{P_x}{b} + \dfrac{P_y}{h}\right) - S \le 0\right\} \ge 1 - [p_{f1}] \\ \quad \Pr\left\{G_2 = \dfrac{4L^3}{E}\sqrt{\left(\dfrac{P_x}{b^3h}\right)^2 + \left(\dfrac{P_y}{bh^3}\right)^2} - D_0 \le 0\right\} \ge 1 - [p_{f2}] \\ \quad 1 \le \mu_b \le 10 \\ \quad 1 \le \mu_h \le 20 \end{cases}$$

Both of the reliability constraint functions are normalized as follows.

$$G_1 = \left[\frac{6L}{bh}\left(\frac{P_x}{b} + \frac{P_y}{h}\right)\right] \Big/ S - 1 \le 0$$

$$G_2 = \frac{4L^3}{E}\sqrt{\left(\frac{P_x}{b^3h}\right)^2 + \left(\frac{P_y}{bh^3}\right)^2} \Big/ D_0 - 1 \le 0$$

The optimal solutions for Case 1 are given in Tables 9 and 10. The solutions from both SORA-FORM and SORA-SPA are almost identical. The probability of failure evaluated by MCS at the optimal points is also the same. The first reliability constraint is active at the optimal solution, and the probability of failure of the first constraint at the optimal point obtained from each of the methods is also displayed in Tables 9 and 10. The second constraint is inactive. Its

probability of failure is much smaller than the required one and is not displayed in the tables. The result indicates that *if all the random variables are normally distributed, both SORA – FORM and SORA – SPA produce the same solution.*

Table 9 Convergence history of SORA-FORM for Case 1

k	f	(μ_b, μ_h)	$g_1^{1-p_{f1}}$	$g_2^{1-p_{f2}}$	p_{f1}	$\varepsilon_{p_{f1}}$	N
1	7.67	(2.06, 3.75)	0.40	0.54			
2	9.58	(2.49, 3.84)	0.0	-0.11	1.04×10^{-3}	4.0%	1351
3	9.58	(2.45, 3.90)	0.0	-0.10			

* The MCS solution p_{f1} is from 10^6 samples, the error of the probability of failure under 95% confidence is 19.2%, and the 95% confidence interval is [0.0008393, 0.0012387].

Table 10 Convergence history of SORA-SPA for Case 1

k	f	(μ_b, μ_h)	$g_1^{1-p_{f1}}$	$g_2^{1-p_{f2}}$	p_{f1}	$\varepsilon_{p_{f1}}$	N
1	7.67	(2.05, 3.75	0.37	0.49			
2	9.56	(2.51, 3.81)	0.0	-0.12	1.04×10^{-3}	4.0%	481
3	9.58	(2.45, 3.91)	0.0	-0.10			

* The MCS solution p_{f1} is from 10^6 samples, the error of the probability of failure under 95% confidence is 19.2%, and the 95% confidence interval is [0.00084113, 0.0012409].

In Case 2, some of the random variables are not normally distributed, the optimal solution from SORA-FORM is different from that of SORA-SPA as shown in Tables 11 and 12. Compared with the confirmation from MCS, the error of the probability of failure associated with the first reliability constraint at the optimal point from SORA-FORM is -62.4% while the error of SORA-SPA is only 0.1%. This indicates that the latter is more accurate than the former when the random variables are not normally distributed. The results for the two cases also show that the efficiency of SORA-SPA is much higher than SORA-FORM.

Table 11 Convergence history of SORA-FORM for Case 2

k	$f(\mathbf{d})$ (in^2)	(μ_b, μ_h) (in)	$g_1^{1-p_{f1}}$	$g_2^{1-p_{f2}}$	p_{f1}	$\varepsilon_{p_{f1}}$	N
1	7.80	(2.02, 3.86)	0.53	0.53			
2	10.35	(2.20, 4.71)	0.0	-0.07	3.760×10^{-4}	-62.4%	1750
3	10.35	(2.20, 4.70)	0.0	-0.07			

* The MCS solution p_{f1} is from 106 samples, the error of the probability of failure under 95% confidence is 31.9%, and 95% confidence interval is [2.558×10^{-4}, 8.032×10^{-4}].

Table 12 Convergence history of SORA-FSPA for Case 2

k	$f(\mathbf{d})$ (in^2)	(μ_b, μ_h) (in)	$g_1^{1-p_{f1}}$	$g_2^{1-p_{f2}}$	p_{f1}	$\varepsilon_{p_{f1}}$	N
1	7.80	(2.02, 3.86)	0.45	0.45			
2	10.07	(2.17, 4.64)	0.02	-0.03	9.99×10^{-4}	0.1%	336
3	10.19	(2.18, 4.67)	0.0	-0.06			
4	10.20	(2.18, 4.67)	0.0	-0.06			

* The MCS solution p_{f1} is from with 10^6 samples, the error the probability of failure under 95% confidence is 19.6%, and 95% confidence interval is [8.03×10^{-4}, 0.0011948].

Example 4 – the design of a two-bar bracket

In this two-bar bracket design problem (Fig. 11), which is adapted from [31], deterministic design variables, random design variables, random parameters, nonnormal distributions, reliability constraints, and deterministic constraints are involved. This is a general problem where all the elements in a RBD model specified in Eq. 1 are included. The details of deterministic design variables $\mathbf{d} = (d_1, d_2, d_3, d_4) = (d_{o1}, d_{i1}, d_{o2}, d_{i2})$, random design variables $\mathbf{X} = (X_1, X_2) = (h, s)$, and random parameters $\mathbf{P} = (P_1, P_2) = (W, \theta, S_1, S_2)$ are given in Table 13. The distributions of all the random variables are given in Table 14.

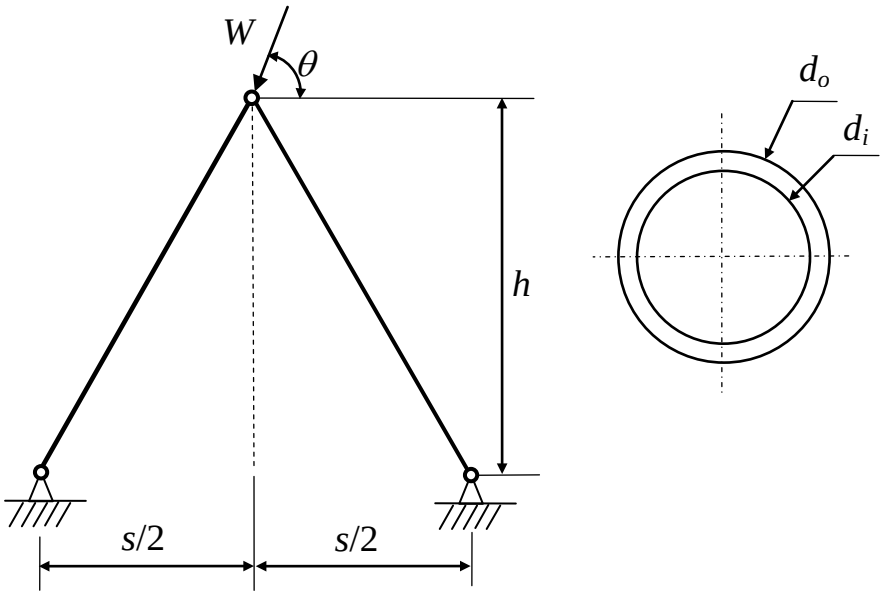

Fig. 11 Two-bar bracket

Table 13 Variables in example 4

Variables	Symbol used in RBD model	Symbol used in Fig. 7	Definition
Deterministic design variables	d_1	d_{o1}	Outer diameter of bar 1
	d_2	d_{i1}	Inner diameter of bar 2
	d_3	d_{o2}	Outer diameter of bar 2
	d_4	d_{i2}	Inner diameter of bar 1
Random design variables	X_1	h	Height of the bracket
	X_2	s	Span of the bracket
Random parameters	P_1	W	External force
	P_2	θ	Angle between W and horizon
	P_3	S_1	Yield strength of bar 1
	P_4	S_2	Yield strength of bar 2

Table 14 Distributions of Random Variables

Variable	Parameter 1*	Parameter 2*	Distribution
h	μ_h mm	5 mm	Normal
s	μ_s mm	5 mm	Normal
θ	58°	62°	Uniform
W	50 kN	5 kN	Extreme type I
S_1	200 MPa	20 MPa	Normal
S_2	200 MPa	20 MPa	Normal

* Parameter 1 is the mean for a normal distribution and extreme type I distribution, and the lower bound for a uniform distribution. Parameter 2 is the standard deviation for a normal distribution and extreme type I distribution, and the upper bound for a uniform distribution

The RBD problem is formulated as

$$
\begin{cases}
\underset{(\mathbf{d},\boldsymbol{\mu}_X)}{\text{Min}}\ f = \dfrac{\pi\rho}{4}\sqrt{\mu_h^2+\left(0.5\mu_s\right)^2}\left(d_{o1}^2-d_{i1}^2+d_{o2}^2-d_{i2}^2\right) \\
\text{s.t.} \\
\Pr\left\{G_1 = 2W\dfrac{\sqrt{h^2+\left(0.5s\right)^2}}{\pi\left(d_{o1}^2-d_{i1}^2\right)}\left(\dfrac{\sin\theta}{h}+2\dfrac{\cos\theta}{s}\right)-S_1\le 0\right\}\ge 1-p_{f1} \\
\Pr\left\{G_2 = 2W\dfrac{\sqrt{h^2+\left(0.5s\right)^2}}{\pi\left(d_{o1}^2-d_{i1}^2\right)}\left(\dfrac{\sin\theta}{h}-2\dfrac{\cos\theta}{s}\right)-S_2\le 0\right\}\ge 1-p_{f2} \\
\Pr\left\{G_3 = -2W\dfrac{\sqrt{h^2+\left(0.5s\right)^2}}{\pi\left(d_{o1}^2-d_{i1}^2\right)}\left(\dfrac{\sin\theta}{h}-2\dfrac{\cos\theta}{s}\right)-S_2\le 0\right\}\ge 1-p_{f3} \\
g_1 = d_{i1}-d_{o1}+0.005\le 0 \\
g_2 = d_{i2}-d_{o2}+0.005\le 0 \\
\mathrm{g}_3 = \mu_s-\mu_h\le 0 \\
0.01\le d_{o1},d_{i1},d_{o2},d_{i2}\le 0.05 \\
0.1\le \mu_h,\mu_s\le 1.0
\end{cases}
$$

The objective is to minimize the volume of the structure, and three probabilistic constraint functions are related to the stresses of the two bars. There are also three deterministic constraint functions. All the reliability constraint functions are also normalized similarly to the treatment in example 3.

The optimal solutions from SORA-FORM and SORA-SPA are displayed in Tables 15 and 16, respectively. The first probabilistic constraint function is active at the optimal points, where the probability of failure is calculated by MCS. The results are given in Table 17, which shows that SORA-SPA is much more accurate and efficient than SORA-FORM.

Table 15 Convergence history of SORA-FORM

k	f (mm^2)	$(d_{o1}, d_{i1}, d_{o2}, d_{i2}, \mu_h, \mu_s)$ (mm)	$g_1^{1-p_f}$	$g_2^{1-p_f}$	$g_3^{1-p_f}$
1	44168.6	(26.75, 19.55, 16.79, 10.79, 101.0, 100.0)	0.66	-0.89	-0.48
2	59541.6	(30.82, 19.94, 15.10, 10.10, 100.0, 100.0)	0.0	-0.85	-0.34
3	59452.1	(25.65, 10.29, 15.0, 10.0, 100.0, 100.0)	0.0	-0.84	-0.33

Table 16 Convergence history of SORA-SPA

k	f (mm^2)	$(d_{o1}, d_{i1}, d_{o2}, d_{i2}, \mu_h, \mu_s)$ (mm)	$g_1^{1-p_f}$	$g_2^{1-p_f}$	$g_3^{1-p_f}$
1	40132.9	(27.64, 20.78, 15.0, 10.0, 100.0, 100.0)	0.56	-0.78	-0.33
2	59543.1	(30.15, 18.93, 15.22, 10.22, 100.0, 100.0)	0.01	-1.09	-0.40
3	59849.8	(30.22, 18.88, 15.0, 10.0, 100.0, 100.0)	0.0	-1.08	-0.38
4	59849.8	(30.22, 18.88, 15.0, 10.0, 100.0, 100.0)	0.0	-1.09	-0.38

Table 17 Probability of failure at the optimal point

Method	p_{f1}	$\varepsilon_{p_{f1}}$	N
SORA-FORM	0.001234	23.4 %	2995
SORA-SPA	0.001055	5.5 %	880

* The MCS solutions p_{f1} are from 10^6 samples. The error of the probability of failure of SORA-FORM under 95% confidence is 17.6%, and the 95% confidence interval is [0.0010164, 0.0014516]. The error of the probability of failure of SORA-SPA under 95% confidence is 19.072%, and the 95% confidence interval is [0.00085379, 0.0012562].

6. Conclusion

The focus of this work is to improve the accuracy of reliability-based design without sacrificing computational efficiency. This is achieved by combining Sequential Optimization and

Reliability Assessment (SORA) and the First Order Saddlepoint Approximation (FOSPA). The proposed method is more accurate than the FORM based RBD methods when the nonnormal-to-normal transformation increases the nonlinearity of probabilistic constraints. Therefore, SORA-SPA can be used as an alternative method to reliability-based design. It should be noted that when all the random variables are normally distributed, SORA-SPA produces exactly the same solutions as FORM-based RBD methods. SORA-SPA may also be extended to the situations where other distribution parameters (such as standard deviations) are part of design variables.

SORA-SPA requires tractable random variables with a closed-form CGF. If all random variables are intractable and are transformed into standard normal variables, the method becomes SORA-FORM. SORA-SPA shares several limitations of FORM based RBD methods. For example, if multiple MLPs exist, SORA-SPA may not provide a correct solution to a RBD problem. Similarly, if a multimodal distribution, which will cause multiple MLPs, is involved, the method may not be applicable. It should also be noted that since SORA-SPA relies on numerical methods such as optimization and MLP search, there is no guarantee of convergence. The other restriction of the current SORA-SPA method is that all the random variables have to be mutually independent. In principle, the Saddlepoint Approximation method is able to handle dependent random variables. The extension of SORA-SPA method to the treatment of dependent random variables should be the future work. The other future work is to investigate the best way to address an intractable random variable and a easy way to determine whether the Saddlepoint Approximation or FORM should be used for a given RBD problem.

Acknowledgements

The support from the U.S. National Science Foundation grant DMI – 040081 and the University of Missouri – Rolla Intelligent Systems Center is gratefully acknowledged. The author would also like to thank anonymous reviewers for their valuable comments and suggestions.

Reference

[1] Zang, T.A., Hemsch, M.J., Hilburger, M.W., Kenny, S.P., Luckring, J.M., Maghami P., Padula, S.L., and Stroud, W. J., 2002, "Needs and Opportunities for Uncertainty-Based Multidisciplinary Design Methods for Aerospace Vehicles," NASA/TM-2002-211462.

[2] Hasofer, A.M. and Lind, N.C., 1974, "Exact and Invariant Second-Moment Code Format," *ASCE Journal of the Engineering Mechanics Division*, **100**(EM1), pp. 111-121.

[3] Wu, Y.-T., Shin, Y., Sues, R., and Cesare, M., 2001, "Safety-Factor Based Approach for Probabilistic-Based Design Optimization," *42nd AIAA/ASME/ASCE/AHS/ASC Structures, Structural Dynamics and Materials Conference and Exhibit*, Seattle, Washington.

[4] Chen, X. and Hasselman, T.K., 1997, "Reliability Based Structural Design Optimization for Practical Applications," *38th AIAA/ASME/ASCE/AHS/ASC Structures, Structural Dynamics and Materials Conference and Exhibit and AIAA/ASME/AHS Adaptive Structural Forum*, Kissimmee, FL.

[5] Du, X. and Chen, W., 2004, "Sequential Optimization and Reliability Assessment method for Efficient Probabilistic Design," *ASME Journal of Mechanical Design*, **126**(2), pp. 225-233.

[6] Du, X, Sudjianto, A., and Huang, B., 2005, "Reliability-Based Design with the Mixture of Random and Interval Variables," *ASME Journal of Mechanical Design*, **127**(6), pp. 1068-1076.

[7] Liang, J., Mourelatos, Z., and Tu, J., 2004, "A Single-Loop Method for Reliability-Based Design Optimization," *2004 ASME International Design Engineering Technical Conferences and Computers & Information In Engineering Conference*, DETC2004-57255, Salt Lake City, Utah.

[8] Wang, L. and Kodiyalam, S., 2002, "An Efficient Method for Probabilistic and Robust Design with Non-normal Distributions," *43rd AIAA/ASME/ASCE/AHS/ASC Structures, Structural Dynamics, and Materials Conference*, Denver, Colorado.

[9] Yang, R. J. and Gu, L., 2004, "Experience with Approximate Reliability-Based Optimization Method," Structural and Multidisciplinary Optimization, **26**(1-2)**,** pp. 152-159.

[10] Yang, R.J., Chuang, C., Gu, L., and Li, G., 2005, "Experience with Approximate Reliability-Based Optimization Methods II: An Exhaust System Problem," Structural and Multidisciplinary Optimization, **29**(6), pp. 488-497.

[11] Der Kiureghian, A., Zhang Y., and Li, C.C., Inverse reliability problem. *Journal of Engineering Mechanics*, 1994, **120**(5), 1150 – 1159.

[12] Tu, J., Choi, K.K., and Young, H.P., 1999, "A New Study on Reliability-Based Design Optimization," *ASME Journal of Mechanical Engineering*, **121**(4), pp.557-564.

[13] Du, X., Sudjianto, A. and Chen, W., 2005, "An Integrated Framework for Optimization under Uncertainty Using Inverse Reliability Strategy," *ASME Journal of Mechanical Design*, **126**, pp. 561-764.

[14] Du, X. and Sudjianto, A., 2004, "The first order saddlepoint approximation for reliability analysis," *AIAA Journal*, **42**(6), pp.1199-1207.

[15] Daniels, H.E., 1954, "Saddlepoint approximations in statistics," *Annals of Mathematical Statistics*, **25**(4), pp.631-650.

[16] Goutis, C. and Casella, G., 1999, "Explaining the saddlepoint approximation," *The American Statistician*, **53**(3), pp.216-224.

[17] Huzurbazar, S., 1999, "Practical Saddlepoint Approximations," *The American Statistician*, **53**(3), pp. 225-232.

[18] Lugannani, R. and Rice, S.O., 1980, "Saddlepoint Approximation for the Distribution of the Sum of Independent Random Variables," *Advances in Applied Probability*, 12, pp. 475-490.

[19] Gatto, R. and Ronchetti, E., 1996, "General Saddlepoint Approximations of Marginal Densities and Tail Probabilities," *Journal of the American Statistical Association*, **91**(433), pp. 666-673.

[20] Wood, A.T.A., Booth, J.G.B., and Butler R.W., 1993, "Saddlepoint Approximations to the CDF of Some Statistics with Nonnormal Limit Distributions," *Journal of the American Statistical Association*, **422**(8), pp. 480-486.

[21] Sudjianto, A., Du, X., and Chen, W., 2005, "Probabilistic Sensitivity Analysis in Engineering Design using Uniform Sampling and Saddlepoint Approximation," SAE 2005 Transactions Journal of Passenger Cars: Mechanical Systems, pp. 267-276.

[22] Jensen, J.L., *Saddlepoint Approximations*, Oxford: Clarendon Press, 1995.

[23] Daniel, H.E., 1987, "Tail probability approximations," *International Statistical Review*, **55**(1), pp.37-48.

[24] Tvedt, L., 1988, "Second order reliability by an exact integral," *Proceedings of the 2nd IFIP WG7.5 Conference*, London, UK, pp. 377-384.

[25] Du, X, Sudjianto, A., 2004, "A Saddlepoint Approximation Method for Uncertainty Analysis," DETC2004-57269, 2004 ASME International Design Engineering Technical Conferences and the Computers and Information in Engineering Conference, Salt Lake City, Utah.

[26] Huang, B. and Du, X., 2005, "Uncertainty Analysis by Dimension Reduction Integration and Saddlepoint Approximations," *ASME Journal of Mechanical Design*, **127**(6), pp.1068-1076.

[27] Johnson, N.L. and Kotz, S., 1970, *Continuous Univariate Distributions-2*, New York: John Wiley and Sons.

[28] Householder, A. S., 1953, *Principles of Numerical Analysis*, New York: McGraw-Hill, pp. 135-138.

[29] Read, K.L.Q., 1998, "A Lognormal Approximation for the Collector's Problem," *The American Statistician*, **52**(2), pp. 179-180.

[30] Huang, B. and Du, X., 2006, "A Saddlepoint Approximation Based Simulation Method for Uncertainty Analysis," *International Journal of Reliability and Safety*, 1(1/2), pp. 206-224.

[31] Arora, J.S., 2004, Introduction to Optimization Design, Elsevier Academic Press, pp. 24-29.